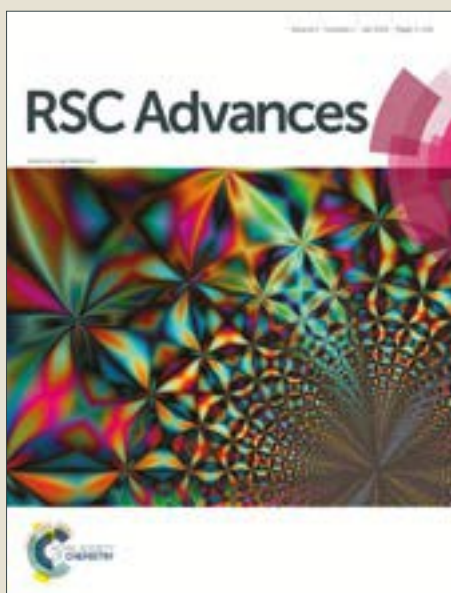


RSC Advances

Accepted Manuscript



This is an Accepted Manuscript, which has been through the Royal Society of Chemistry peer review process and has been accepted for publication.

Accepted Manuscripts are published online shortly after acceptance, before technical editing, formatting and proof reading. Using this free service, authors can make their results available to the community, in citable form, before we publish the edited article. We will replace this Accepted Manuscript with the edited and formatted Advance Article as soon as it is available.

You can find more information about Accepted Manuscripts in the [author guidelines](#).

Please note that technical editing may introduce minor changes to the text and/or graphics, which may alter content. The journal's standard [Terms & Conditions](#) and the ethical guidelines, outlined in our [author and reviewer resource centre](#), still apply. In no event shall the Royal Society of Chemistry be held responsible for any errors or omissions in this Accepted Manuscript or any consequences arising from the use of any information it contains.

Influence of electrodes types on the electrohydrodynamic instability patterning process: a comparative study

Minzhe Liu^{1,2}, Hefu Li¹, Weixing Yu^{3,*}, Taisheng Wang¹, Zhenyu Liu¹ and Marc. P. Y. Desmulliez^{4,*}

This article studies the effect that different types of patterned electrodes have on the electrohydrodynamic instability patterning (EHDIP) process for the faithful replication of micro- and nanostructures. Two types of patterned electrodes are studied. One is fully conductive, i.e. both pattern and substrate are conductive. The other type has conductive microstructures fabricated on a dielectric substrate. By employing the COMSOLTM Multiphysics software package, a rigorous numerical simulation of the EHDIP process has been carried out for both types of electrodes. The simulation results show that both electrodes can realize a faithful replication of the micro- and nanostructures once the variable, $\Delta E/\Delta x$, reaches the critical value. Moreover, it is demonstrated that a fully conductive template is preferred if a small polymer film thickness is employed; a partially conductive electrode is preferred for larger film thickness. These results provide guidelines for the better control of EHDIP process in order to realize the perfect pattern replication of structures for a variety of applications in MEMS or micro/nanofluidics.

Introduction

Electrohydrodynamic patterning, as a novel lithographic technique, employs capillary thin film instability for the manufacture of micro- and nano-scale structures. When a liquid film is subjected to a uniform electric field, the electrical stress at surface of the film generates periodical pillars with space equal to the largest unstable wavelength under some conditions¹⁻⁷. The competition between electrostatic stress and capillary effects determines a characteristic wavelength λ , which is proportional to $\gamma^{1/2}H^{3/2}V^{-1}$, where γ is the interfacial tension, V the voltage applied to the electrode, and H is the separation between the top and bottom electrode. Due to its potential applications for making micro- and nano-scale structures economically and efficiently, a lot of experimental⁸⁻²⁶ and theoretical²⁷⁻³⁰ studies have been carried out and show the onset of instability in a viscous film when the electrical force dominates over the stabilizing surface tension force. Recently, full numerical simulations were developed to explain the dynamic behavior of the EHDIP process and to provide insights for the intelligent design of templates to produce long range ordered patterns³¹⁻³⁷.

To obtain certain types of ordered patterns, the application of a spatially varying electric field by using a topologically structured electrode was also reported as a useful means of controlling the lateral dimensions of the microstructures^{28,31,33,37}. The patterned electrode modulates the electric field spatially, which has a two-fold influence on the development of the surface instability. The instability is directed towards the template protrusions by the pressure gradients that are induced by the height variations of the template. In addition, the protruding structures of the template lead to an increased electric field strength that leads to a locally increased growth rate of the instability. As a result, a positive replica of the structure in electrode is obtained.

In order to manufacture grating patterns in thin film, methods include the utilization of a patterned conducting surface as a master template^{1,7,18,22}, of dielectric patterns on a conductive substrate^{10,24,26} and of patterns in conductive material on a dielectric substrate²⁵. Compared with the type of conductive patterns on a dielectric substrate, the other two types have stronger modulation of the spatial distribution of the electric field, which helps to guarantee the faithful replication in thin film easily. So the two types of patterned electrodes are studied emphatically in this article by employing the COMSOLTM Multiphysics software package. A faithful replication of patterns in the underlying polymer film is determined by the interplay of the two lateral length scales that are intrinsic to the EHDIP process. One lateral length scale is the aforementioned characteristic wavelength λ . The other length scale is the periodicity of the patterned master electrode on the substrate. In this case, the periodicity of the pattern is greater than the largest unstable wavelength. Periodic pillars or replica of the template due to the coalescence of periodic pillars

¹ State Key Laboratory of Applied Optics, Changchun Institute of Optics, Fine Mechanics & Physics, Chinese Academy of Sciences, No.3888, Dongnanhu Road, Changchun, Jilin, P.R.China.

² University of the Chinese Academy of Science, Beijing, 100049, P.R. China

³ Key Laboratory of Spectral Imaging Technology, Xi'an Institute of Optics and Precision Mechanics, Chinese Academy of Sciences, No.17, Xixi Road, Xian 710119, P. R. China. E-mail: ywx@opt.ac.cn

⁴ MicroSystems Engineering Centre (MISEC), School of Engineering & Physical Sciences, Heriot-Watt University, Edinburgh EH14 4AS, UK. Fax: +44 (0)131 451 4155; Tel: +44 (0)131 451 3340; E-mail: m.desmulliez@hw.ac.uk

can also be formed in the film. In that case, the periodicity of the pattern on template is smaller than the largest unstable wavelength and disorder structures will be formed due to the relatively weaker gradients induced by the patterned template³⁶. Therefore, a greater lateral gradient in the electric field is needed to guarantee the faithful replica of the template in the film.

One notable question needs to be addressed here is how to design the optimum pattern electrode so that a strong enough spatially modulated electric field can be obtained to realize the faithful replication of patterns in the film. Normally, a fully conductive template (pattern and substrate) is used as the master electrode. Here, we propose a new type of partially conductive template consisting of conductive patterns on a dielectric substrate. The schematic drawing of the experimental sandwich-like configuration is sketched in Figure 1. Consider a polymer film surrounded by air resting on a planar substrate under the influence of a heterogeneous electric field. Figure 1(A) shows a patterned electrode and planar substrate, both electrically conductive. Figure 1(B) shows the conductive patterns on a dielectric substrate. For a patterned mask, the height of the electrode protrusions, the width of the electrode protrusions, and the period of the grating mask are denoted by p , w and l , respectively. The master electrode applied with voltage u is positioned above the substrate at distance d .

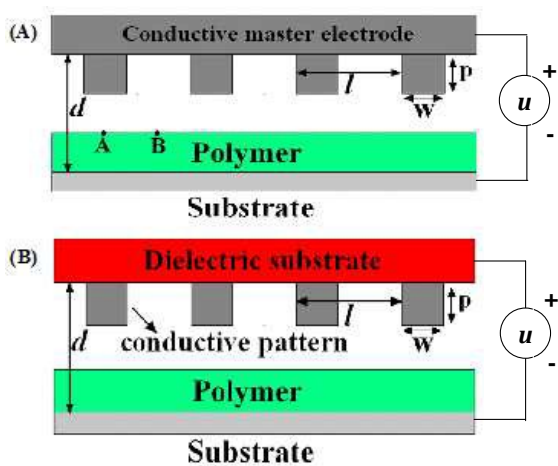


Figure 1: Schematic diagrams of a polymer film resting on a planar substrate under the influence of a heterogeneous electric field. (A) A conductive patterned electrode. (B) A conductive pattern on a dielectric substrate.

The template shown in Figure 1(B) has a stronger modulation of the spatial distribution of the electric field. A stronger lateral gradient in the electric field distribution results in additional flow and overcomes the spinodal effects, which

helps to guarantee the faithful replication in thin film. To further understand the advantages of partial conductive template over the traditional fully conductive template, a numerical model of the EHDIP process has been developed by employing the COMSOLTM Multiphysics software package (Version 4.3). Based on the model, we demonstrate that micro- and nanostructures can be realized easily. Furthermore, it is found that, under some conditions, partially conductive template is more effective in comparison with the traditional fully conductive template. The numerical simulation results provide useful guidelines for the experimental work to achieve the faithful fabrication of micro/nanostructures by applying the optimum process parameters.

Model Analysis

The evolution equation of the free surface, derived from the Navier-Stokes equation and continuity equation in the long wave limit, governs the dynamics of a thin liquid film subjected to an external electric field

$$\frac{\partial h}{\partial t} = \frac{\partial}{\partial x} \left[\frac{h^3}{3\mu} \left(\frac{\partial p}{\partial x} \right) \right] \quad (1)$$

In equation (1), h is the local thickness of the film at the position x ; t is the time; μ is the viscosity of the film. P , the total pressure at the interface in the film, can be defined as

$$P = P_0 - \gamma \nabla^2 h + P_{el}(h) \quad (2)$$

Where P_0 is the ambient pressure. The second term in the right hand side of the equation is the Laplace pressure introduced by the curvature of the film. The third term, P_{el} , is the electrostatic pressure, defined as

$$P_{el} = -0.5 \epsilon_0 \epsilon_r (\epsilon_r - 1) E_p^2 \quad (3)$$

$$E_p = \frac{u}{\epsilon_r d - (\epsilon_r - 1)h} \quad (4)$$

Where E_p is the electric field strength in the polymer film; ϵ_0 is the dielectric permittivity of the vacuum; ϵ_r is the relative dielectric constant of the polymer film; u is the applied voltage and d is the separation distance between the template and the substrate.

Assuming a periodic pattern for the template, the generated electric field will be spatially modulated. The electric field strength distribution at the film at the initial stage will therefore follow a sinusoidal profile and can be decomposed into a Fourier series²⁵:

$$E_p = E_0 + \sum_{n=1}^{+\infty} E_n e^{-d/\frac{w}{2\pi n}} \cos \frac{2\pi nx}{w} \quad (5)$$

E_0 is the mean value of the electric field. The second term on the right-hand side of equation (5) is the varying component of the electric field. w is the periodicity of the features on the template; E_n is the electric field intensity of the n^{th} harmonic in the Fourier series.

In general, the large value of pressure gradient ensures a faithful replication of the pattern in the underlying polymer film^{27,30,37}. With reference to Figure 1, the difference of internal pressure of polymer film between point A, a peak in the field distribution, and point B, a valley, is the difference of electrostatic pressure between point A and point B, as the atmospheric and Laplace pressures at both points are the same. The equations 1-5 provide the calculation method of the electric field strength in the polymer film and the electric field strength at point A and B are E_A and E_B separately. Thus, a parameter, $\Delta E/\Delta x$, can be defined between points A and B, to characterize the effect of the difference of electrostatic pressure on the growth of the polymer film, with the aim to qualitatively measure the effect of the varying electric field on the EHDIP process,

$$\frac{\Delta E}{\Delta X} = \frac{E_A - E_B}{X_B - X_A} \quad (6)$$

Where Δx is the distance between A and B. The value is disparate for different templates. As $\Delta E/\Delta x$ increases, the effect of the modulating electric field on the film increases. This effect can suppress the homogeneous field instability and result in the formation of a faithful replication. Because the electrical field distribution is influenced by the electrical properties of the template, the value of $\Delta E/\Delta x$ for fully conductive patterned electrode and partial conductive patterned electrode is different even with the same structural parameters. Different manufacturing limit can be obtained for a given template with different electrical conductivities.

Numerical Method

Figure 1 shows the geometry of the problem and the initial configuration: a film coated on the substrate. For reasons of periodicity only four periods are modeled. Properties of the polymer liquid used in the simulation are presented in Table 1.

| Density (kg/m ³) | Simulated dynamic (Pa·S) | Dielectric constant | Surface tension (N/m) |
|---------------------------------|--------------------------------|------------------------|-----------------------------|
| 1000 | 1 | 2.5 | 0.038 |

Table 1. Properties of the material used in the simulations.

In this simulation, the Level Set Two-Phase Flow application module and electrostatics module found in the COMSOLTM Multiphysics software package are adopted. Navier-Stokes equation and continuity equation have to be considered^{6,33,37}.

$$\rho \frac{\partial V}{\partial t} + \rho(V \cdot \nabla)V = -\nabla p + \nabla \cdot (\mu \nabla V) + \mathbf{F} \quad (7)$$

$$\frac{\partial \rho}{\partial t} + \nabla \cdot (\rho V) = 0 \quad (8)$$

In the equation, V is the flow velocity vector, P , ρ and μ are respectively the pressure, density and kinematic viscosity of each fluid. \mathbf{F} , the volume force, is caused by the atmospheric pressure P_0 . The surface tension $\mathbf{F}_{st} = \sigma \kappa \delta \mathbf{n}$, and the electrostatic pressure P_0 , and is denoted by $\mathbf{F} = (P_0 + \sigma \kappa + P_e) \delta \mathbf{n}$, where σ is the surface tension coefficient (N/m), κ is the curvature, δ is a delta function concentrated to the surface, and \mathbf{n} is the unit vector pointing outward perpendicularly to the interface.

To track and follow the evolution of the interface between the two fluids (liquid and air), we use the level set method, which has proven popular in recent years for tracking, modeling and simulating the motion of moving interface or boundaries. Where the interface between the two fluids is represented by the 0.5 contour of the level set function ϕ , which is in the range of 0 to 1. A smeared out Heavisides function is used with $\phi < 0.5$ for one phase and as $\phi > 0.5$ for the other and the transition is varied smoothly across the interface. δ smoothens the surface tension which is concentrated at the interface between fluids and is approximated according to the relation

$$\delta = |\nabla \phi| |\phi(1-\phi)| \quad (9)$$

The interface normal and the interface curvature are determined by Eq. (10) and Eq. (11) respectively.

$$\mathbf{n} = \frac{\nabla \phi}{|\nabla \phi|} \quad (10)$$

$$\kappa = -\nabla \cdot \left(\frac{\nabla \phi}{|\nabla \phi|} \right) \quad (11)$$

The electric field is solved by using the Laplace equation for the voltage assuming that there is zero free charge in the bulk fluid:

$$\nabla \cdot \nabla u = 0 \quad (12)$$

The interface moves with the fluid, whose flow velocity vector, V is described by the following equation:

$$\frac{\partial \phi}{\partial t} + V \cdot \nabla \phi = \gamma \nabla \cdot \left(\varepsilon \nabla \phi - \phi (1 - \phi) \frac{\nabla \phi}{|\nabla \phi|} \right) \quad (13)$$

Where γ is the stabilization parameter; ε is the parameter that controls the interface thickness and should have the same order of magnitude as the computational mesh size of the elements where the interface propagates. The parameters γ and ε determine the thickness of the region and the amount of re-initialization or stabilization of the level set function, respectively. The density and viscosity are calculated from

$$\rho = \rho_1 + (\rho_2 - \rho_1)\phi \quad (14)$$

$$\mu = \mu_1 + (\mu_2 - \mu_1)\phi \quad (15)$$

Where ρ_1 and ρ_2 are the fluid densities of the air and polymer film. The parameters μ_1 and μ_2 indicate the dynamic viscosities of the air and the polymer film. This model is solved by the finite elements method embedded into the software package.

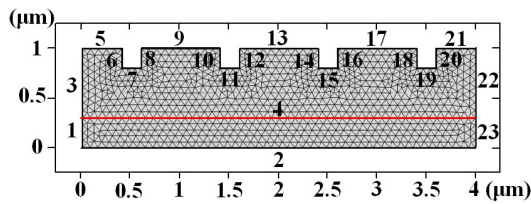


Figure 2: Schematic diagram introducing the geometry, boundary condition and mesh of the two-dimension model. The red line is the air-film interface. Dimension unit is μm .

Figure 2 shows the geometry, boundary conditions and mesh of the two-dimension model in the case of four periods of the pattern. For a conductive patterned electrode, a DC voltage is applied between the bottom (boundary 2) and the top electrode with electrical potential (boundaries 5, 6, 7...19, 20 and 21). For a partially conductive electrode, the boundaries 5, 9, 13, 17 and 21 are set to be at zero potential, other boundary conditions are similar to those of a conductive patterned electrode. The boundary conditions for the fluid flow are: (a) no slip at boundaries 2, 5, 6, 7...19, 20 and 21; (b) periodic boundary at boundaries 1, 3, 22 and 23; (c) initial fluid interface at boundary 4. In order to simulate a periodic structure, it is necessary to introduce the periodic boundary condition at boundaries 1, 3, 22 and 23. The sources 1 and 3 corresponding to the destinations 23 and 22, respectively. The expressions for the sources are the pressure in the fluid P and the flow velocity vector V .

Results and Discussions

The influence of the film thickness with the fully conductive electrode has been studied³⁷. The results show that the faithful replication can be completed when the initial film thickness is changed from 0.3 to 0.5 μm . When the film thickness is smaller or larger, the replication of grating microstructures is unsuccessful. In this article, we use the same template as shown in Figure 1 to study the effect that the two types of patterned electrodes have on the electrohydrodynamic instability patterning (EHDIP) process for the faithful replication of microstructures. We chose different film thickness of 0.3, 0.4 and 0.5 μm . According to the equation(4), the voltage is proportional to the film thickness. So the voltages set for different film thicknesses are different to guarantee the faithful replication.

The detailed evolution of the electrically induced patterning process with patterned conductive template is shown in Figure 3. Simulation results show a two-dimensional periodic microstructure induced by a conductive patterned electrode with protrusion height of 0.2 μm and width of 0.2 μm . The period l of the protrusion is 1 μm . The gap d between the electrodes is 1 μm . The initial polymeric film thickness is 0.3 μm . The applied DC voltage on the top electrode is 230 V and the bottom electrode is grounded. At the start, the polymer film surface is flat as shown in Figure 3A. As the spatial heterogeneity of the electrostatic field induced by the patterned top electrode increases, the polymer liquid grows upwards firstly under the protrusion of the top electrode due to the higher electric field as shown in Figure 3B. The resulting uplifted polymer experiences a greater electrostatic force as the polymer approaches the top electrode, pulling the polymer fluid further towards the protrusion of the top electrode as represented in Figure 3C. The growing polymer touches the surface of the top electrode, and is stopped from moving further upwards, forming structures similar to the pattern on the template as shown in Figure 3D.

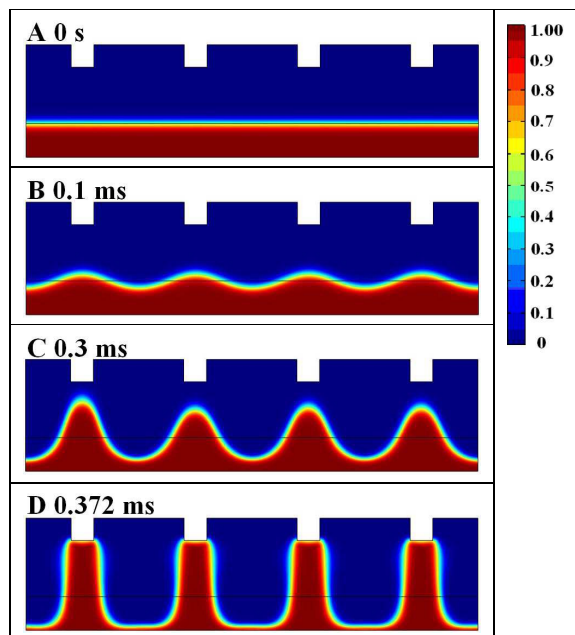


Figure 3: Spatiotemporal evolution of a 0.3 μm thick polymer liquid interface. Red colour represents the polymer liquid, and the blue colour represents air.

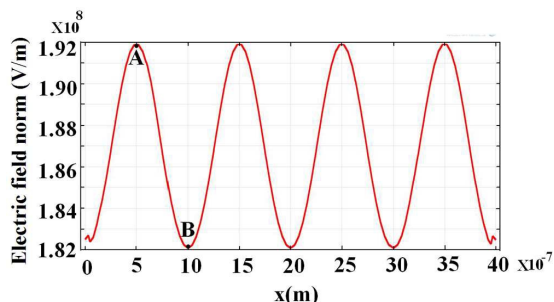


Figure 4: Initial electric field strength located at the surface of the polymer film in the EHDIP process as shown in Figure 3.

Figure 4 shows the initial electric field strength distribution at the air/polymer interface. As can be seen, the electric field distribution follows a sinusoidal profile. The electric field strength underneath the center of the protrusion (Point A) is much larger than that in other areas. The electric field strength underneath the center of the cavity (Point B) is the smallest. Accordingly, the internal pressure at this point is smaller than those in other areas.

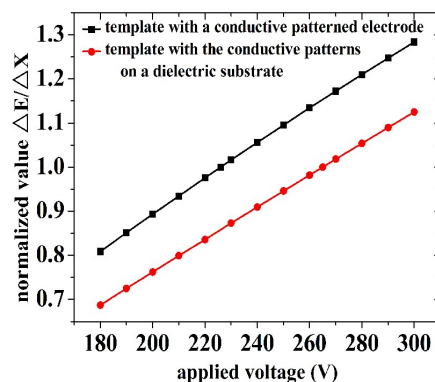


Figure 5: Dependence of the normalized variable $\Delta E/\Delta X$ on the applied voltage u for the case $w=0.2 \mu\text{m}$, and $p=0.2 \mu\text{m}$. $h_0=0.3 \mu\text{m}$ and $d=1 \mu\text{m}$.

Figure 5 shows the relationship between the normalized variable $\Delta E/\Delta X$ and the applied voltage when the polymer film thickness is 0.3 μm . For convenience, the parameter $\Delta E/\Delta X$ is normalized by dividing this quantity by the critical $\Delta E/\Delta X$ defined as the minimum value needed to be reached to obtain faithful replication in the underlying polymer film can be realized. The critical $\Delta E/\Delta X$ value for a fully conductive template is $1.98 \cdot 10^{13} \text{ Vm}^{-2}$ when the applied voltage is 226 V where it is $9.37 \cdot 10^{13} \text{ Vm}^{-2}$ for the partial conductive template and an applied voltage is 265 V. Therefore, if the normalized $\Delta E/\Delta X$ equals 1, the applied voltage is 226 V for conductive template and is 265 V for partial conductive template, respectively. Increasing the voltage helps improving the modulation of electrical field. It is also clear that a lower applied voltage than in the partially conductive template is needed to achieve the same gradient of electric field for conductive template. The conductive template is therefore preferred for this condition.

A detailed comparison of the EHDIP process for different types of template is reported in Figure 6. Figure 6A shows the induced structures in polymer under the heterogeneous electric field generated by a conductive patterned electrode when the value of the applied voltage is 226 V. As is shown in Figure 6A, the pattern from the master electrode is well replicated by the polymeric film. However, if the voltage is increased to 265 V as shown in Figure 6B, the uniformity of the replicated pattern in the film is better than that of Figure 6A. If the master electrode is changed to be partially conductive and without changing any other process parameters, the EHDIP evolution process is rather different. As is shown in Figure 6C, there is only one column well replicated in the polymeric film. In this

case, the voltage needs to be increased larger than 265 V to realize the replication of the pattern in polymer as shown in Figure 6D. In general, the results reveal that the fully conductive electrode performs better in comparison with the partially conductive electrode when a lower necessary applied voltage is provided.

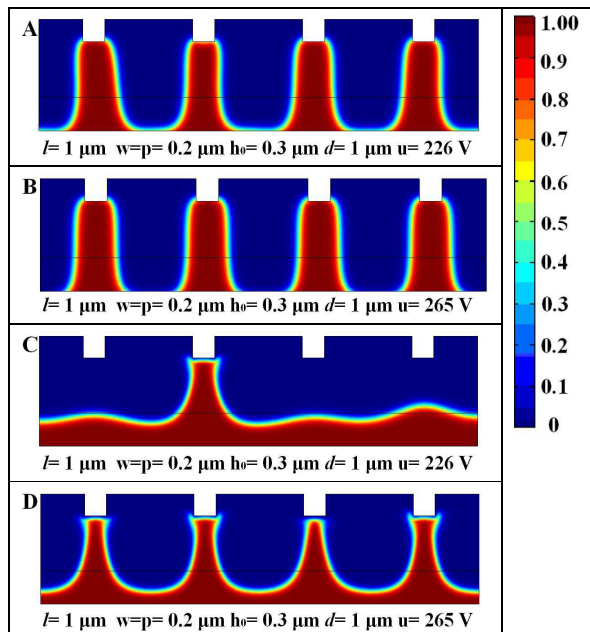


Figure 6: EHDIP spatio-temporal evolution results for different types of templates and voltages. The film thickness is 0.3 μm . Red color represents the polymer liquid; blue represents air.

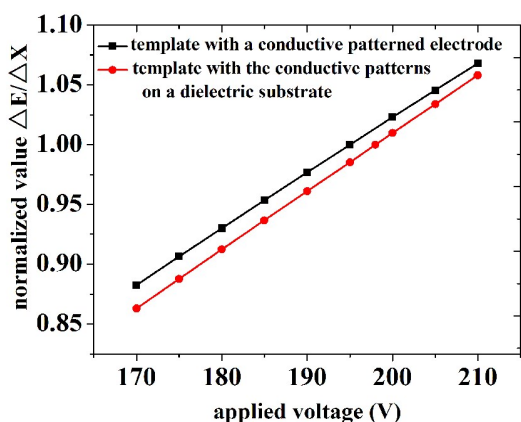


Figure 7: Variation of $\Delta E/\Delta X$ as a function of the applied voltage u for the case $w=0.2 \mu\text{m}$, and $p=0.2 \mu\text{m}$. $h_0=0.4 \mu\text{m}$ and $d=1 \mu\text{m}$.

Figure 7 shows the relationship between the normalized variable $\Delta E/\Delta X$ and the applied voltage when the polymer film thickness is 0.4 μm . The critical value of $\Delta E/\Delta X$ for the conductive template is $3.44 \times 10^{13} \text{ Vm}^{-2}$ for a voltage of 195 V

and $1.32 \times 10^{14} \text{ Vm}^{-2}$ for the partially conductive template for a voltage of 198 V. The geometric structure resembles that of Figure 3. In this case, it is clear that conductive template is preferable to the partially conductive template as a lower voltage is possible to realize the faithful replication.

The detailed comparison of the EHDIP process for different types of the template when film thickness is 0.4 μm can be seen in Figure 8. Figure 8A shows the induced structures in polymer under the heterogeneous electric field generated by a conductive patterned electrode for an applied voltage of 195 V. The pattern from the master electrode is well replicated by the polymeric film. For an increased value of applied voltage to 198 V as shown in Figure 8B, the uniformity of the pattern replica in the film is improved. However, if the master electrode is changed to be partially conductive, without changing other process parameters, the EHDIP evolution process is rather different. As is shown in Figure 8C, there is only one pillar formed. When the voltage is increased to 198 V in Figure 8D, a fair replication of the master can be achieved. In general, the results revealed that the fully conductive electrode performs slightly better than with the partially conductive electrode in terms of necessary applied voltage.

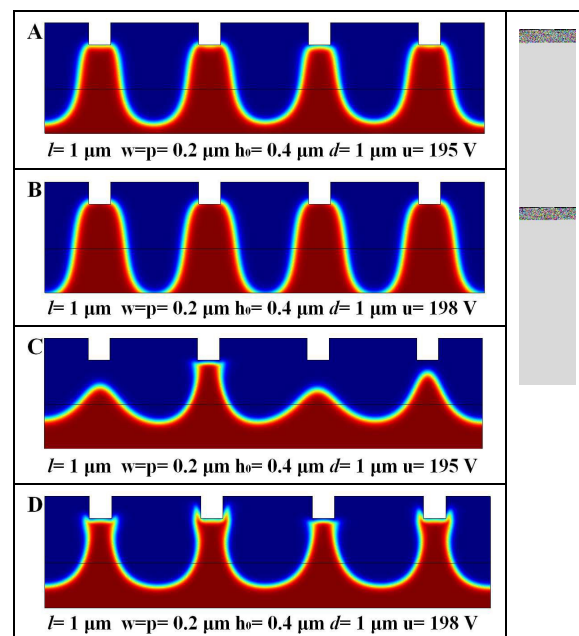


Figure 8: EHDIP spatio-temporal evolution results for different types of template and voltage when film thickness is 0.4 μm . Red colour represents the polymer liquid, and the blue colour represents air.

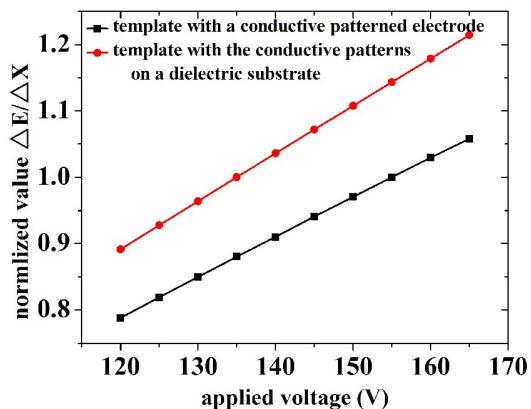


Figure 9: Evolution of $\Delta E/\Delta X$ of as a function of the applied voltage u for the case $w=0.2 \mu\text{m}$, and $p=0.2 \mu\text{m}$. $h_0=0.5 \mu\text{m}$ and $d=1 \mu\text{m}$.

Figure 9 shows the relationship between the normalized variable $\Delta E/\Delta X$ and the applied voltage when the polymer film thickness is $0.5 \mu\text{m}$. Again, increasing the applied voltage always helps to achieve the replica of the master. In this case, the critical value of $\Delta E/\Delta X$ for the conductive template is $5.7 \cdot 10^{13} \text{Vm}^{-2}$ for a voltage of 155V and $1.73 \cdot 10^{14} \text{Vm}^{-2}$ a voltage of 135V in the partially conductive case.

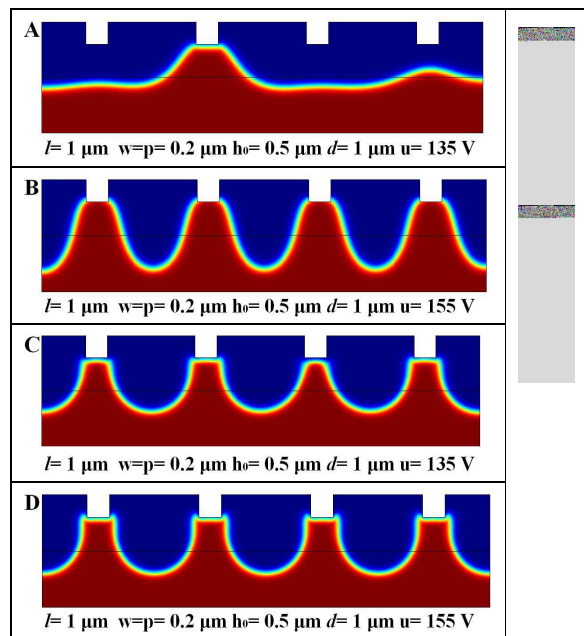


Figure 10: EHDIP spatio-temporal evolution results for different types of template and voltage when film thickness is $0.5 \mu\text{m}$. Red colour represents the polymer liquid, and the blue colour represents air.

The detailed comparison of the EHDIP process for different

types of the template when film thickness is $0.5 \mu\text{m}$ can be seen in Figure 10. Figure 10A shows that only unordered structures emerge at the surface of the polymer with a voltage of 135V for patterned conductive electrode. When the applied voltage is increased to 155V , the perfect replication of the pattern is realized as shown in 10B. However, as shown in Figure 10C, only 135V is needed for a partially conductive patterned electrode to realize the perfect replication. If the voltage is increased to 155V as shown in Figure 10D, the uniformity of the replicated pattern in the film is better than that of Figure 10C. In general, the results indicate that the partially conductive electrode performs better in comparison with the fully conductive electrode in terms of the lower necessary applied voltage.

Moreover extensive numerical simulations predict that different types of template have their own advantages depending on the film thickness. Compared with other technological parameters, the film thickness is much easier to be controlled experimentally. Thus, we study the effect of the film thickness specially for the formation of the microstructures. As is shown by above simulation results, fully conductive template is preferred for smaller film thickness and partial conductive template is preferred for larger film thickness.

Conclusions

In summary, the EHDIP process can realize a faithful replication when the variable, $\Delta E/\Delta X$, reaches a critical value. If the critical value of $\Delta E/\Delta X$ meets the requirement, larger voltage helps to achieve a better replication. Some similar experiments are conducted. The article³⁸ demonstrates the faithful transfer of patterns with a high aspect ratio onto a polymer film via electrohydrodynamic instabilities for a given patterned grating mask. In the experiment, grating structures can be obtained when the film thickness is set at 16 and $23 \mu\text{m}$, which is consistent with the rule of chosen the film thickness mentioned previously. In addition, experimental results show a better replication can be achieved when the voltage is increased to 150V , which is consistent with the simulation results. In general, a fully conductive template is preferred for smaller film thickness and a partially conductive template is preferred for larger film thickness. These results shed some light on the structure optimization of the electrode for the EHDIP process to realize the perfect pattern replication.

Acknowledgments

The authors acknowledge the financial support from Natural Science Foundation of China under grant numbers

61361166004, 61475156, 61490712 and 51275504 as well as the financial support from Science and Technology Development Plane of Jilin under grant numbers 20140519002JH and 20140519007JH. The authors acknowledge also the financial support from the Engineering & Physical Research Council (EPSRC) through the UK Innovative electronic Manufacturing Research Centre (IeMRC) which awarded the Flagship project entitled “Smart Microsystems” (FS/01/02/10).

Bibliographical references

- 1 Eric Schäffer, Thomas Thurn-Albrecht, Thomas P. Russell, Ullrich Steiner, *Nature*, 2000, **403**, 874-877.
- 2 Nicoleta E. Voicu, Stephan Harkema, and Ullrich Steiner, *Adv. Funct. Mater.*, 2006, **16**, 926-934.
- 3 K. Amanda Leach, Zhiqun Lin, and Thomas P. Russell, *Macromolecules*, 2005, **38**, 4868 – 4873.
- 4 Zhiqun Lin, Tobias Kerle, Thomas P. Russell, Eric Schäffer and Ullrich Steiner, *Macromolecules*, 2002, **35**, 3971 – 3976.
- 5 Zhiqun Lin, Tobias Kerle, Shenda M. Baker, David A. Hoagland, Eric Schäffer and Ullrich Steiner, Thomas P. Russell, *J. Chem. Phys.*, 2001, **114**, 2377-2381.
- 6 Eric Schäffer, Thomas Thurn-Albrecht, Thomas P. Russell, Ullrich Steiner, *Europhys. Lett.*, 2001, **53**, 518-524.
- 7 Mihai D. Morariu, Nicoleta E. Voicu, E. Schäffer, Zhiqun Lin, T.P. Russell and U. Steiner, *Nature Materials*, 2002, **2**, 48-52.
- 8 Paru Deshpande, Xiaoyun Sun, and Stephen Y. Chou, *Applied Physics Letters*, 2001, **79**, 1688-1690.
- 9 Hongqi Xiang, Yao Lin, and Thomas P. Russell, *Macromolecules*, 2004, **37**, 5358 – 5363.
- 10 Stephan Harkema and Ullrich Steiner, *Adv. Funct. Mater.*, 2005, **15**, 2016-2020.
- 11 Ning Wu, Leonard F. Pease, III, and William B. Russel, *Adv. Funct. Mater.*, 2006, **16**, 1992-1999.
- 12 Narasimhan Arun, Ashutosh Sharma, Vijay B. Shenoy and K. S, *Adv. Mater.*, 2006, **18**, 660-663.
- 13 Joonwon Bae, Elizabeth Glogowski, Suresh Gupta, Wei Chen, Todd Emrick and Thomas P. Russell, *Macromolecules*, 2008, **41**, 2722 – 2726.
- 14 Leonard F. Pease, III and William B. Russel, *Langmuir*, 2004, **20**, 795 – 804.
- 15 N. Arun, Ashutosh Sharma, Partho S. G. Pattader, Indrani Banerjee, Hemant M. Dixit and K. S. Narayan, *Physical Review Letters*, 2009, **102**, (254502-1)-(254502-4).
- 16 K. Amanda Leach and Suresh Gupta, Michael D. Dickey, C. Grant Willson, Thomas P. Russell, *CHAOS*, 2005, **15**, 047506.
- 17 Michael D. Dickey, Suresh Gupta, K. Amanda Leach, Elizabeth Collister, C. Grant Willson, Thomas P. Russell, *Langmuir*, 2006, **22**, 4315 – 4318.
- 18 G Liu, W Yu, H Li, J Gao, D Flynn, R W Kay, S Cargill, C Tonry, M K Patel, C Bailey and M P Y Desmulliez, *J. Micromech. Microeng.*, 2013, **23**, 035018.
- 19 Stephen Y. Chou and Lei Zhuang, *J. Vac. Sci. Technol. B.*, 1999, **17**, 3197-3202.
- 20 Lin Wu, and Stephen Y. Chou, *Applied Physics Letters*, 2003, **85**, 3200-3202.
- 21 Stephen Y. Chou; Lei Zhuang; and Linjie Guo, *Applied Physics Letters*, 1999, **75**, 1004-1006.
- 22 Xinya Lei, Lin Wu, Paru Deshpande, Zhaoning Yu, Wei Wu, Haixiong Ge and Stephen Y Chou, *Nanotechnology*, 2013, **14**, 786-790.
- 23 V. Shankar and Ashutosh Sharma, *Journal of Colloid and Interface Science*, 2004, **274**, 294-308.
- 24 Nicoleta E. Voicu, M. S. M. Saifullah, K. R. V. Subramanian, Mark E. Welland, and Ullrich Steiner, *Soft Matter*, 2007, **3**, 554-557.
- 25 Xin Li, Jinyou Shao, Yucheng Ding, Hongmiao Tian, Hongzhong Liu, *J. Micromech. Microeng.*, 2011, **21**, 1-7.
- 26 Jakob Heier, Jan Groenewold and Ullrich Steiner, *Soft Matter*, 2009, **5**, 3997-4005.
- 27 R. V. Craster, O. K. Matar, *Physics of fluids*, 2005, **17**, 032104.
- 28 Scott A. Roberts and Satish Kumar, *Physics of fluids*, 2010, **22**, 122102.
- 29 F. Li, O. Ozen, N. Aubry, D. T. Papageorgiou and P. G. Petropoulos, *J. Fluid Mech.*, 2007, **583**, 347-377.
- 30 Gaurav Tomar, V. Shankar, Ashutosh Sharma, Gautam Biswas, *J. Non-Newtonian Fluid Mech.*, 2007, **143**, 120-130.
- 31 Ning Wu, Leonard F. Pease III, and William B. Russel, *Langmuir*, 2005, **21**, 12290 – 12302.
- 32 Dongchoul Kim and Wei Lu, *PHYSICAL REVIEW B*, 2006, **73**, 035206.
- 33 H. Li, W. Yu, L. Zhang, Z. Liu, K.E. Brown, E. Abraham, S. Cargill, C. Tonry, M.K. Patel, C. Bailey and M.P.Y. Desmulliez, *RSC Adv.*, 2013, **3**, 11839-11845
- 34 Jayati Sarkar and Ashutosh Sharma, Vijay B. Shenoy, *Physical Review E*, 2008, **77**, 031604.
- 35 Dipankar Bandyopadhyay, Ashutosh Sharma, Uwe Thiele, and P. Dinesh Sankar Reddy, *Langmuir*, 2009, **25**, 9108-9118.
- 36 Ruhi Verma; Ashutosh Sharma; Kajari Kargupta; Jaita Bhaumik, *Langmuir*, 2005, **21**, 3710-3721.
- 37 H. Li, W. Yu, Y. Wang, H. Bu, Z. Liu, E. Abraham, M. P. Y, *RSC Advances*, 2014, **4**, 13774.
- 38 H Li, W Yu, T Wang, H Zhang, Y Cao, E Abraham, M. P. Y, *J. Micromech. Microeng.*, 2014, **24**, 075006.